

Nonequilibrium Response Theory: From Precision Limits to Strong Perturbation

Ruicheng Bao^{1,*} and Shiling Liang (梁师翎)^{2,3,4,†}

¹*Department of Physics, Graduate School of Science, 7-3-1,
The University of Tokyo, Hongo, Bunkyo-ku, Tokyo 113-0033, Japan*

²*Center for Systems Biology Dresden, 01307 Dresden, Germany*

³*Max Planck Institute for the Physics of Complex Systems, 01187 Dresden, Germany*

⁴*Max Planck Institute of Molecular Cell Biology and Genetics, 01307 Dresden, Germany*

Fluctuation-response relations lie at the heart of statistical physics, yet their formulation in nonequilibrium steady states remains challenging. This Letter makes two key contributions to this field: First, we establish fundamental limits on nonequilibrium steady-state responses by deriving upper bounds on response precisions using steady-state Fisher information. Our analysis reveals that the sensitivity of observables to perturbations is governed by mean first passage times, steady-state currents, and activities, though it cannot be enhanced indefinitely by increasing these quantities. Notably, we demonstrate that the role of activity in response precision parallels that of repeated measurements in metrology. Second, we develop novel identities connecting the responses to arbitrarily strong perturbations with those to small perturbations. These identities significantly extend previous nonequilibrium response theories, which primarily focused on small perturbations, to encompass arbitrarily strong perturbations.

Introduction.— Fluctuation-response relations are cornerstones of statistical physics, fundamentally linking a systems' intrinsic fluctuations to its response to external perturbations. While fluctuation-dissipation theorems provide a complete framework near equilibrium [1], real-world systems such as biological systems operate far from equilibrium to achieve functions like signal processing and biochemical regulation [2–4], necessitating new theoretical tools for both fluctuations and responses in nonequilibrium settings.

Recent advances in stochastic thermodynamics have established a powerful framework for analyzing nonequilibrium systems subject to thermal fluctuations [5]. On the relation between fluctuation and response, general inequalities for both stationary and non-stationary cases were derived in [6] using stochastic trajectories and information theory. A parallel route uses algebraic graph theory to build thermodynamic bounds on steady-state responses [7–10]. More recently, identities and thermodynamic bounds were developed for response in nonequilibrium steady states, ranging from responses of steady-state distribution, currents to general observables [6, 11–17].

Despite these developments, a comprehensive framework for the response of nonequilibrium steady state remains incomplete. Firstly, existing non-equilibrium fluctuation-response bounds mainly focus on trajectory-wise observables [6, 11–13, 15, 17–19]. Such observables are generically resource-intensive to evaluate in experiments. In contrast, state observables, which are time-intensive and more experimentally accessible in the sense that their statistical moments take less time to converge in sampling for experiments and simulations, remain largely unexplored. Second, while most approaches are

limited to small perturbations, with few studies touching finite perturbation bounds [6, 20], practical applications often involve finite perturbations [21, 22]. A general framework for treating such finite perturbations is still lacking.

In this Letter, we establish two main results for nonequilibrium response theory to address these challenges. First, by determining the Fisher information associated with steady-state distributions of Markov jump processes, we derive general upper bounds on response precision expressed through mean first passage times, currents, and activities. These bounds provide experimentally accessible estimates for entropy production (EP) and cycle affinity. Second, we derive novel identities connecting finite and small perturbation responses, extending nonequilibrium response theories beyond the linear regime. Together, these results provide a unified framework for analyzing both weak and strong perturbations, with broad implications for thermodynamic inference [23–25].

Setup.— We consider a continuous-time Markov process with N discrete states. The dynamics of the system is determined by a transition rate matrix W whose off-diagonal element W_{ij} denotes the transition rate on the edge e_{ij} from state j to state i . Its diagonal elements are defined as $W_{ii} = -\sum_{j(\neq i)} W_{ji}$. Assuming that W is irreducible and aperiodic ensures the existence of a unique steady-state probability distribution $\boldsymbol{\pi} = (\pi_1, \dots, \pi_N)^T$ satisfying

$$W \cdot \boldsymbol{\pi} = \mathbf{0}.$$

To formalize perturbations and responses, we parametrize the transition rates following [6, 7] as

$$W_{ij} = e^{-(B_{ij} - E_j - F_{ij}/2)} \quad (1)$$

where E_j is the vertex parameter, $B_{ij} = B_{ji}$ is the symmetric edge parameter and $F_{ij} = -F_{ji}$ is the asymmetric

* Corresponding author: ruicheng@g.ecc.u-tokyo.ac.jp

† Corresponding author: shiling@pks.mpg.de

ric edge parameter. Physically, these parameters describe a system within an energy landscape with wells of depth E_j , energy barrier of height B_{ij} , and driving force F_{ij} . For a cycle in the network, one can define the cycle affinity as the sum of driving forces along the cycle, $F_c = \sum_{e_{ij} \in c} F_{ij}$. The system is out-of-equilibrium when there exists at least one cycle with non-zero cycle affinity. In what follows, we study the response of physical observables in the system to perturbations on these parameters.

Steady-state fluctuation-response theory— Then, we introduce the mean first passage time (MFPT) of the system from an arbitrary state j to state i as $\langle t_{ij} \rangle > 0$ when $i \neq j$. We artificially define $t_{ii} = 0$ instead of as the mean first return time of state i . Based on a relation between the response and the MFPT [26–28] (θ is an arbitrary parameter associated with the transition matrix),

$$\frac{d \ln \pi_k}{d\theta} = \sum_{i,j(i \neq j)} \pi_j \frac{dW_{ij}}{d\theta} (\langle t_{kj} \rangle - \langle t_{ki} \rangle), \quad (2)$$

we show that for single-edge perturbation,

$$\frac{\partial \ln \pi_k}{\partial B_{mn}} = -(\langle t_{kn} \rangle - \langle t_{km} \rangle) j_{mn}, \quad (3a)$$

$$\frac{\partial \ln \pi_k}{\partial F_{mn}} = (\langle t_{kn} \rangle - \langle t_{km} \rangle) \frac{A_{mn}}{2}, \quad (3b)$$

where $j_{mn} = W_{mn}\pi_n - W_{nm}\pi_m$ is the steady state probability current from state n to state m and $A_{mn} = W_{mn}\pi_n + W_{nm}\pi_m$ is the edge activity of e_{mn} . Additionally, a known result of vertex perturbation [7] can also be recovered from Eq. (2) as

$$\frac{\partial \ln \pi_k}{\partial E_m} = \pi_m - \delta_{km}, \quad (4)$$

where δ_{km} is the Kronecker delta. Here, $\sum_i W_{ij} \langle t_{ki} \rangle = \delta_{jk} / \pi_j - 1$ and $\sum_i W_{ij} = 0$ have been used.

To proceed, we calculate the Fisher information, a quantity that can provide the optimal performance of the response of a given steady state $\boldsymbol{\pi}$. For our system, the Fisher information of perturbing a parameter θ associated with the steady state $\boldsymbol{\pi}$ is given by

$$I(\theta) := \sum_i \pi_i \left(\frac{\partial \ln \pi_i}{\partial \theta} \right)^2 \quad (5)$$

Equipped with the definition and the single-edge perturbation, we get that

$$\sqrt{I(B_{mn})} = |j_{mn}| \sqrt{\sum_k \pi_k (\langle t_{km} \rangle - \langle t_{kn} \rangle)^2}, \quad (6a)$$

$$\sqrt{I(F_{mn})} = \frac{A_{mn}}{2} \sqrt{\sum_k \pi_k (\langle t_{km} \rangle - \langle t_{kn} \rangle)^2}, \quad (6b)$$

$$\sqrt{I(E_m)} = \sqrt{\pi_m (1 - \pi_m)}. \quad (6c)$$

The Cramer-Rao bound $\frac{(\partial_\theta \langle \mathcal{O} \rangle)^2}{\text{Var}(\mathcal{O})} \leq I(\theta)$ yields upper bounds for response precision:

$$\frac{|\partial_{B_{mn}} \langle \mathcal{O} \rangle_\pi|}{\sqrt{\text{Var}_\pi(\mathcal{O})}} \leq |j_{mn}| \sqrt{\sum_k \pi_k (\langle t_{km} \rangle - \langle t_{kn} \rangle)^2}, \quad (7a)$$

$$\frac{|\partial_{F_{mn}} \langle \mathcal{O} \rangle_\pi|}{\sqrt{\text{Var}_\pi(\mathcal{O})}} \leq \frac{A_{mn}}{2} \sqrt{\sum_k \pi_k (\langle t_{km} \rangle - \langle t_{kn} \rangle)^2}, \quad (7b)$$

$$\frac{|\partial_{E_m} \langle \mathcal{O} \rangle_\pi|}{\sqrt{\text{Var}_\pi(\mathcal{O})}} \leq \sqrt{\pi_m (1 - \pi_m)}. \quad (7c)$$

Here, $\langle \mathcal{O} \rangle_\pi := \sum_i \mathcal{O}_i \pi_i$ is the steady-state average of an arbitrary observable \mathcal{O} and $\text{Var}_\pi(\mathcal{O}) := \sum_i (\mathcal{O}_i - \langle \mathcal{O} \rangle_\pi)^2 \pi_i$ is its steady-state variance. The response precision of \mathcal{O} to the perturbation on a parameter θ is naturally quantified by the ratio from response strength $|\partial_\theta \langle \mathcal{O} \rangle|$ to the intrinsic fluctuation characterized by $\sqrt{\text{Var}(\mathcal{O})}$. Note that steady-state average and variance of an observable are experimentally feasible. In contrast, the steady-state distribution is typically not due to coarse-graining. These upper bounds may provide design principles for optimal responses and sensing in biological and chemical systems: The kinetic asymmetry characterized by difference in MFPTs constrains the optimal performance of sensing state observables.

Intuitively, the difference between two MFPTs, the edge activity A_{mn} and the steady-state current J_{mn} can all be arbitrarily large, implying the response precision may be arbitrarily enhanced by increasing these quantities. However, using two inequalities

$$\left| \frac{\partial \ln \pi_k}{\partial F_{mn}} \right| \leq (1 - \pi_k), \quad (8a)$$

$$\left| \frac{\partial \ln \pi_k}{\partial B_{mn}} \right| \leq (1 - \pi_k) \tanh(F_{\max}^{(m,n)}/4) \quad (8b)$$

derived in [7], we show that the MFPT difference, steady-state currents and the activity are upper bounded as

$$|\langle t_{km} \rangle - \langle t_{kn} \rangle| \frac{A_{mn}}{2} \leq 1 - \pi_k \leq 1, \quad (9a)$$

$$|\langle t_{km} \rangle - \langle t_{kn} \rangle| |j_{mn}| \leq (1 - \pi_k) \tanh(F_{\max}^{(m,n)}/4), \quad (9b)$$

where $F_{\max}^{(m,n)}$ is the cycle affinity maximized over all cycles containing the perturbed edge e_{mn} . The physical meaning of Eq. (9a) and Eq. (9b) are that if the activity or current in edge (m, n) are larger, state m and n are more kinetically indistinguishable. For activity, imagine that A_{mn} is very large, then the system will jump between m and n for many times within a time unit, so that the difference in MFPT from these states to any other states will be very small. For current, if there is a very large j_{mn} , then whenever the system is in m or n , it will most likely go to or stay in m , eliminating the kinetic difference between them. Moreover, when $k = m$, i.e., the focused edge is perturbed, we

have $\langle t_{mn} \rangle \leq \min\left\{\frac{2}{A_{mn}}, \frac{\tanh(F_{\max}^{(m,n)}/4)}{|j_{mn}|}\right\}$, which allow us to bound an arbitrary MFPT. These observations reveal the key physics behind the ultimate limits of response precision, as shown below.

Ultimate limits of response precision for state observables.— Combining Eq. (7a), Eq. (7b), Eq. (9a) and Eq. (9b), we conclude that the response precision for steady-state distribution is limited as

$$\frac{|\partial_{B_{mn}}\langle\mathcal{O}\rangle_\pi|}{\sqrt{\text{Var}_\pi(\mathcal{O})}} \leq \left(1 - \frac{1}{N}\right) \min\left\{\tanh(F_{\max}^{(m,n)}/4), \frac{2|j_{mn}|}{A_{mn}}\right\}, \quad (10a)$$

$$\frac{|\partial_{F_{mn}}\langle\mathcal{O}\rangle_\pi|}{\sqrt{\text{Var}_\pi(\mathcal{O})}} \leq \left(1 - \frac{1}{N}\right) \min\left\{1, \frac{A_{mn} \tanh(F_{\max}^{(m,n)}/4)}{2|j_{mn}|}\right\}, \quad (10b)$$

$$\frac{|\partial_{E_m}\langle\mathcal{O}\rangle_\pi|}{\sqrt{\text{Var}_\pi(\mathcal{O})}} \leq \sqrt{\pi_m(1 - \pi_m)} \leq \frac{1}{2}, \quad (10c)$$

where $\sqrt{\sum_k \pi_k(1 - \pi_k)^2} \leq 1 - 1/N$ has been used. With $\tanh(x) \leq 1$, these ultimate limits demonstrate that the intrinsic performance of state-observable response cannot be larger than $1 - \frac{1}{N}$. This implies that the response precision of state observables is not related to timescale (activity) of the system, in contrast with trajectory observables. Eq. (9a)-(9b) and Eq. (10a)-(10c) constitute our first main result.

Eq. (10a)-(10b) not only reflect thermodynamic constraints on response but also offer experimentally feasible bounds for maximal cycle affinity and EP rate (EPR). The bounds for EPR are obtained as

$$\frac{\dot{\sigma}_{mn}}{A_{mn}} \geq \frac{(\partial_{B_{mn}}\langle\mathcal{O}\rangle_\pi)^2}{\text{Var}_\pi(\mathcal{O})[\sum_k \pi_k(1 - \pi_k)^2]} \geq \frac{(\partial_{B_{mn}}\langle\mathcal{O}\rangle_\pi)^2}{\text{Var}_\pi(\mathcal{O})(1 - \frac{1}{N})^2}, \quad (11)$$

where $\dot{\sigma}_{mn} < \dot{\sigma}$ is the steady-state EPR associated with the perturbed edge. $\frac{\dot{\sigma}_{mn}}{A_{mn}}$ can be interpreted as the EP per transition in e_{mn} . A_{mn} can be obtained by counting the average number of transitions in edge (m, n) per time unit. Thus, using Eq. (11), one can obtain an estimation of EPR by observing non-directed transitions on a single edge and a rough observable \mathcal{O} without knowing dynamical details of other parts of the system. This lower bound uses only time-symmetric observables which are time-intensive, in contrast with current-type observables or counting observables used in the celebrated thermodynamic uncertainty relations [29–36].

For multiple edge perturbations, the corresponding response precision is at most proportional to the number of the perturbed edges (Appendix B).

Response of currents.— Using Eq. (2), we derive exact expressions for steady-state current responses and their upper bounds. For non-local perturbations where $e_{mn} \neq$

e_{kl} , we have

$$\frac{\partial j_{mn}}{B_{kl}} = -[\Delta t_{lk}^n \mathcal{T}_{nm} - \Delta t_{lk}^m \mathcal{T}_{mn}] j_{kl}, \quad (12a)$$

$$\frac{\partial j_{mn}}{F_{kl}} = [\Delta t_{lk}^n \mathcal{T}_{nm} - \Delta t_{lk}^m \mathcal{T}_{mn}] \frac{A_{kl}}{2}, \quad (12b)$$

$$\frac{\partial j_{mn}}{E_k} = \pi_k j_{mn}, \quad (12c)$$

where $\Delta t_{lk}^n := \langle t_{nl} \rangle - \langle t_{nk} \rangle$. For local perturbations,

$$\frac{\partial j_{kl}}{B_{kl}} = j_{kl}(-1 + \langle t_{kl} \rangle \mathcal{T}_{lk} + \langle t_{lk} \rangle \mathcal{T}_{kl}), \quad (13a)$$

$$\frac{\partial j_{kl}}{F_{kl}} = \frac{1}{2} A_{kl} [1 - (\langle t_{kl} \rangle \mathcal{T}_{lk} + \langle t_{lk} \rangle \mathcal{T}_{kl})] \quad (13b)$$

$$\frac{\partial j_{kl}}{E_k} = \pi_k A_{kl} + j_{kl}. \quad (13c)$$

Then, using Eqs. (9a)-(9b) we can obtain upper bounds for non-local and local current response as (for simplicity, we only take B_{kl} as an example)

$$\left| \frac{\partial j_{mn}}{B_{kl}} \right| \leq \min\left\{\tanh(F_{\max}^{(k,l)}/4), \frac{2|j_{kl}|}{A_{kl}}\right\} A_{mn}. \quad (14a)$$

$$\left| \frac{\partial j_{kl}}{B_{kl}} \right| \leq \min\left\{A_{kl} \tanh(F_{\max}^{(k,l)}/4), |j_{kl}|\right\} \leq A_{kl}. \quad (14b)$$

Thus, the single-edge response for an arbitrary current observable (generalized current) $\langle \mathcal{J} \rangle := \sum_{m < n} \mathcal{J}_{mn} j_{mn}$ can be upper bounded as

$$\frac{d\langle \mathcal{J} \rangle}{dB_{kl}} \leq \sum_{m < n} \mathcal{J}_{mn} A_{mn}. \quad (15)$$

Unlike steady-state distributions and state observables, current response is more intrinsically linked to activity. Eq. (14a)-(15), show that higher activity leads to enhanced responses in both currents and current observables. This occurs because current observables inherently depend on jump frequencies, while state observables only depend on residence times. However, we define a type of measurable normalized current observable $\langle \mathcal{J} \rangle^{nom} := \sum_{m < n} \mathcal{J}_{mn} (p_{mn} \pi_n - p_{nm} \pi_m)$ by introducing the next-state probability,

$$p_{mn} := p(x_1 = m | x_0 = n) = \frac{W_{mn}}{|W_{nn}|} \quad (m \neq n),$$

with x_0 and x_1 representing the states before and after a transition ($p_{mm} := 0$). We show that their response precision is upper bounded by 2, similar to the state observables (Appendix C).

Nonequilibrium response theory for arbitrarily-strong perturbations.— We begin by generalizing Eq. (2) to cases where the perturbation can be arbitrarily strong (Appendix A):

$$\pi'_k - \pi_k = \sum_{m < n} (\langle t_{kn} \rangle - \langle t_{km} \rangle) (\Delta W_{mn} \pi'_n - \Delta W_{nm} \pi'_m) \pi_k, \quad (16)$$

where $\Delta W_{mn} = W'_{mn} - W_{mn}$ is the perturbation and π'_k is the steady state probability of state k for perturbed dynamics. A discrete-time version of Eq. (16) was derived in [26]. We remark that the discrete-time result cannot be transformed into Eq. (16) by normalizing transition rates of the continuous-time process. We also note that Eq. (16) was recently derived in [37] using a different approach. As a byproduct, we get a new duality equation of Eq. (16) as

$$\pi'_k - \pi_k = \sum_{m < n} (\langle t'_{kn} \rangle - \langle t'_{km} \rangle) (\Delta W_{mn} \pi_n - \Delta W_{nm} \pi_m) \pi'_k, \quad (17)$$

where $\langle t'_{kn} \rangle$ denotes the MFPT of the perturbed dynamics. Both Eq. (16) and Eq. (17) reduce to Eq. (2) in the weak perturbation limit ($|\Delta W_{mn}| \ll 1$ for all m, n).

Using Eq. (16), we obtain the finite-perturbation counterparts of Eq. (3a) - (4) as

$$\frac{\pi_k^{B'_e} - \pi_k^{B_e}}{1 - e^{\Delta B_e}} = (\langle t_{kn} \rangle - \langle t_{km} \rangle) \pi_k j_{mn}^{B'_e}, \quad (18a)$$

$$\frac{\pi_k^{F'_e} - \pi_k^{F_e}}{1 - e^{-\Delta F_e/2}} = (\langle t_{km} \rangle - \langle t_{kn} \rangle) \pi_k \left(\mathcal{T}_{nm}^{F'_e} + e^{\Delta F_e/2} \mathcal{T}_{mn}^{F'_e} \right), \quad (18b)$$

$$\frac{\pi_k^{E'_m} - \pi_k^{E_m}}{e^{\Delta E_m} - 1} = \pi_m^{E'_m} (\pi_k^{E_m} - \delta_{km}) \quad (18c)$$

where $\mathcal{T}_{nm} := W_{nm} \pi_m$, $\Delta B_e = B'_e - B_e$ and $\Delta F_e = F'_e - F_e$ (for notation brevity, we denote $e = e_{mn}$, $B_e := B_{mn}$, $F_e := F_{mn}$ and $j_e := j_{mn}$ from now on). Then, we obtain linear relations between responses of state observables to strong and weak perturbation as

$$\frac{\langle \mathcal{O} \rangle_{\pi}^{B'_e} - \langle \mathcal{O} \rangle_{\pi}^{B_e}}{e^{\Delta B_e} - 1} = \frac{j_e^{B'_e}}{j_e^{B_e}} \partial_{B_e} \langle \mathcal{O} \rangle_{\pi}^{B_e}, \quad (19a)$$

$$\frac{\langle \mathcal{O} \rangle_{\pi}^{F'_e} - \langle \mathcal{O} \rangle_{\pi}^{F_e}}{1 - e^{-\Delta F_e/2}} = \frac{\mathcal{T}_{nm}^{F'_e} + e^{\Delta F_e/2} \mathcal{T}_{mn}^{F'_e}}{A_e^{F_e}} \partial_{F_e} \langle \mathcal{O} \rangle_{\pi}^{F_e} \quad (19b)$$

$$\frac{\langle \mathcal{O} \rangle_{\pi}^{E'_m} - \langle \mathcal{O} \rangle_{\pi}^{E_m}}{e^{\Delta E_m} - 1} = \frac{\pi_m^{E'_m}}{\pi_m^{E_m}} \partial_{E_m} \langle \mathcal{O} \rangle_{\pi}^{E_m}, \quad (19c)$$

Eq. (19a)-(19c) comprise our second main result. Our derivation of Eq. (16) relies solely on the steady-state condition and the existence of a generator pseudoinverse, and is thus not limited to Markov jump processes. Linear relations similar to Eq. (19a)-(19c) may be found for other dynamical equations.

These identities enable us to generalize previous nonequilibrium response theories from weak perturbation to arbitrarily strong perturbation. For instance,

the fluctuation-response relations for state observables derived in [38] are extended to:

$$\text{Cov}[\mathcal{O}_1, \mathcal{O}_2] = \sum_e \frac{A_e}{(j_e^{B'_e})^2} \left(\frac{\Delta_{B_e} \langle \mathcal{O}_1 \rangle}{e^{\Delta B_e} - 1} \right) \left(\frac{\Delta_{B_e} \langle \mathcal{O}_2 \rangle}{e^{\Delta B_e} - 1} \right), \quad (20a)$$

$$= \sum_e \frac{A_e \left[\frac{\Delta_{F_e} \langle \mathcal{O}_1 \rangle \Delta_{F_e} \langle \mathcal{O}_2 \rangle}{(1 - e^{-\Delta F_e/2})^2} \right]}{\left(\mathcal{T}_{nm}^{F'_e} + e^{\Delta F_e/2} \mathcal{T}_{mn}^{F'_e} \right)^2} \quad (20b)$$

where $\Delta_{B_e} \langle \mathcal{O} \rangle := \langle \mathcal{O} \rangle_{\pi}^{B'_e} - \langle \mathcal{O} \rangle_{\pi}^{B_e}$. When ΔB_e and ΔF_e are small, relations in [38] are recovered. Combining Eq. (20a) with the Cauchy-Schwartz inequality, we obtain

$$\min_e \left(\frac{A_e}{A'_e} \right) \sum_e \frac{\left(\frac{\Delta_{B_e} \langle \mathcal{O} \rangle}{e^{\Delta B_e} - 1} \right)^2}{\langle \langle \mathcal{O} \rangle \rangle} \leq \dot{\sigma}'_{ps} \leq \dot{\sigma}'. \quad (21)$$

Note that the covariance and the variance $\langle \langle \mathcal{O} \rangle \rangle$, which have the dimension of time, are defined in [38]. If the perturbation is to increase B_e , then $|j_e|$ will decrease [13], while the cycle affinity is unchanged. In this case, $\dot{\sigma}' \leq \dot{\sigma}$, so that Eq. (21) provides a feasible lower bound for the EPR. Other fluctuation-response inequalities for state observables in [15, 38] can be extended with the same logic.

Eq. (4), (8a) and (8b) can be generalized similarly to upper bound $|\pi_k^{X'_e} - \pi_k^{X_e}|$ and $|\Delta_{X_e} \langle \mathcal{O} \rangle|$, where $X_e = B_e, F_e, E_e$. Our results on the ultimate response of state observables are also generalizable to finite perturbations by substituting Eq. (19a)-(19c) into Eq. (10a)-(10c). If one wants to consider the variances before and after the perturbations, an inequality first derived in [11, 17] can be applied (Appendix D).

For steady-state currents j_{mn} , finite perturbation counterparts of Eq. (12a) and Eq. (13a) are derived as (F_{kl} and E_m are similar)

$$\frac{j_{mn}^{B'_e} - j_{mn}^{B_e}}{1 - e^{\Delta B_e}} = -[\Delta t_{lk}^n \mathcal{T}_{nm} - \Delta t_{lk}^m \mathcal{T}_{mn}] j_{kl}^{B'_e}, \quad (22a)$$

$$\frac{j_{kl}^{B'_e} - j_{kl}^{B_e}}{1 - e^{-\Delta B_e}} = j_{kl}^{B_e} \left[-1 - \frac{j_{kl}^{B'_e}}{j_{kl}^{B_e}} (\langle t_{kl} \rangle \mathcal{T}_{lk} + \langle t_{lk} \rangle \mathcal{T}_{kl}) \right]. \quad (22b)$$

Comparing Eq. (12a), Eq. (13a) with Eq. (22a) and Eq. (22b), we find that for non-local current responses, the linearity holds similarly to steady-state probability:

$$\frac{j_{mn}^{B'_e} - j_{mn}^{B_e}}{1 - e^{\Delta B_e}} = \frac{j_{kl}^{B'_e}}{j_{kl}^{B_e}} \frac{\partial j_{mn}^{B_e}}{\partial B_e}, \quad (23)$$

which is, however, not the case for local perturbations. Consequently, linearity in Eq. (19a)-(19c) does not hold for current observables $\langle \mathcal{J} \rangle$.

Example: Biochemical sensing—To illustrate our bounds in a biologically relevant context, we analyze a minimal push-pull network motif ubiquitous in cellular signaling pathways. The system transitions between inactive (X) and active (X^*) states via two competing enzyme-catalyzed reactions with rates $w_{\pm} = e^{E_{X/X^*} - B_w \pm F_w/2}$ and $k_{\pm} = e^{E_{X/X^*} - B_k \pm F_k/2}$. This interconversion can represent various post-translational modifications like phosphorylation-dephosphorylation that are crucial for cellular information processing [8, 39]. Operating out of equilibrium with steady-state probabilities $[\pi_X, \pi_{X^*}]$, the system has a single cycle of affinity $F_c = F_w - F_k$. Our bounds on the response precision for any observable \mathcal{O} reduce to: $\frac{|\partial_{B_w} \langle \mathcal{O} \rangle_{\pi}|}{\sqrt{\text{Var}_{\pi}(\mathcal{O})}} < \tanh(F_c/4)/2$, $\frac{|\partial_{F_w} \langle \mathcal{O} \rangle_{\pi}|}{\sqrt{\text{Var}_{\pi}(\mathcal{O})}} \leq 1/2$ and $\frac{|\partial_{E_{X^*}} \langle \mathcal{O} \rangle_{\pi}|}{\sqrt{\text{Var}_{\pi}(\mathcal{O})}} \leq 1/2$. These bounds place fundamental thermodynamic constraints on how strongly an observable can respond to parameter changes relative to its intrinsic fluctuations. Our numerical tests verify these limits for random observables and system parameters, as shown in Fig. 1.

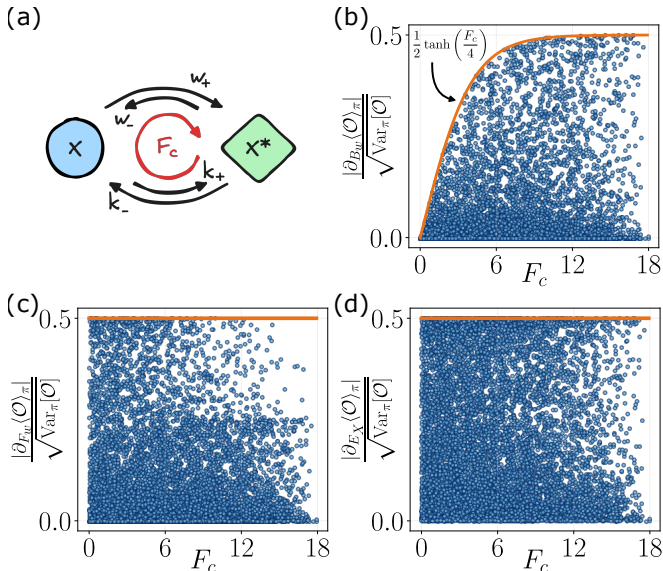


FIG. 1. (a) Minimal push-pull signaling motif where a substrate interconverts between inactive (X) and active (X^*) states with rates w_{\pm} and k_{\pm} , maintained out of equilibrium with cycle affinity F_c . (b-d) Numerical verification of bounds on response precision under different perturbations: (b) symmetric edge parameter (B_w), (c) asymmetric edge parameter (F_w), and (d) vertex parameter (E_X). Blue dots show numerical results for random observables and parameters; orange lines indicate theoretical bounds. For B_w perturbations, the bound scales as $\tanh(F_c/4)/2$, while for F_w and E_X , a constant bound of $1/2$ applies.

Discussions.— We present a comprehensive framework for understanding and optimizing the response behaviors of nonequilibrium steady states. Our contributions are twofold. First, we develop a nonequilibrium response theory based on steady-state Fisher information, revealing

fundamental bounds for response precision. Notably, our findings elucidate the role of activity in nonequilibrium response: while higher activity enables more frequent repeated measurements, thereby enhancing measurement precision of the mean value, it does not improve the intrinsic precision for state observables. From a metrological perspective, our variance is the single-measurement variance, capturing the intrinsic fluctuations of state observables. In contrast, variances of such observables in the very recent [15, 38] are tied to activity (repeated measurements) and have the dimension of time.

Second, we extend the nonequilibrium response theory beyond the weak-perturbation regime to encompass arbitrary perturbation strengths by establishing equalities between responses to strong and weak perturbations. This generalization makes the nonequilibrium response theory more applicable to practical experiments.

Looking forward, it would be valuable to extend our theory to systems governed by Lindblad master equations. Additionally, addressing different classes of perturbations, such as time-dependent signals commonly encountered in biological systems [40, 41], represents an important direction for future work.

ACKNOWLEDGMENTS

R. B. was supported by JSPS KAKENHI. We are grateful to the Statistical Physics Youth Communication community for providing the initial platform for this discussion. We also acknowledge the assistance of Claude and ChatGPT for their help with writing, critical comments, and inspiring discussions.

APPENDIX

Appendix A: Mean first passage time, Drazin pseudoinverse and response

We provide the definitions of MFPT and Drazin pseudoinverse of rate matrix, and an explicit expression of the MFPT using Drazin pseudoinverse of the rate matrix. The MFPT from state j to state i is defined as

$$\langle t_{ij} \rangle = \int_0^{\infty} t_{ij} f(t_{ij}) dt_{ij}, \quad (24)$$

where t_{ij} is the random first passage time and $f(t_{ij})$ is its probability density function. t_{ij} is a random variable defined as

$$t_{ij} := \inf_{t \geq 0} \{X(t) = i | X(0) = j\}.$$

Here, $X(t)$ is the state of the system at time t . That is, t_{ij} is the first time at which a stochastic trajectory reaches state i at time t , given that it starts from state j

at time 0. The MFPT has a closed-form expression using the Drazin pseudoinverse [28, 42],

$$\langle t_{ij} \rangle = \frac{W_{ij}^{\mathcal{D}} - W_{ii}^{\mathcal{D}}}{\pi_i}, \quad (25)$$

which will be used later. The Drazin pseudoinverse $W^{\mathcal{D}}$ of a rate matrix W is defined as the matrix satisfying following conditions [43]:

$$\begin{aligned} W^{\mathcal{D}} W W^{\mathcal{D}} &= W^{\mathcal{D}}, \\ W^{\mathcal{D}} W &= W W^{\mathcal{D}}, \\ W W^{\mathcal{D}} W &= W. \end{aligned}$$

A useful property of $W^{\mathcal{D}}$ is [43]

$$W^{\mathcal{D}} W = \mathbb{I} - \boldsymbol{\pi} \mathbf{e}, \quad (26)$$

where \mathbb{I} is a $N \times N$ identity matrix, $\boldsymbol{\pi}$ is written as a column vector and $\mathbf{e} = (1, \dots, 1)$ is a row vector with all N elements being 1. A possible choice of $W^{\mathcal{D}}$ is

$$W^{\mathcal{D}} = (\mathbb{I} - \boldsymbol{\pi} \mathbf{e}) \int_0^{\infty} (e^{Wt} - \boldsymbol{\pi} \mathbf{e}) dt.$$

In what follows, we derive Eq. (16), then Eq. (2) holds as a specific case. We realize that Eq. (2) was first derived in [28], and an equivalent form of it was recently re-derived in [38, 44], without identifying the MFPT from Drazin pseudoinverse.

We denote the transition rate matrices before and after an arbitrarily strong perturbation as W and W' . Similarly, column vectors $\boldsymbol{\pi}$ and $\boldsymbol{\pi}'$ are the steady-state probability distribution before and after the perturbation. Observe that

$$W(\boldsymbol{\pi}' - \boldsymbol{\pi}) = -(W' - W)\boldsymbol{\pi}' \quad (27)$$

because of the steady-state condition $W\boldsymbol{\pi} = \mathbf{0}$ and $W'\boldsymbol{\pi}' = \mathbf{0}$. We aim to express the finite response $\boldsymbol{\pi}' - \boldsymbol{\pi}$ using the perturbation $W' - W$ on transition rate matrix, so that the W on the left should be put to the right. Since W is invertible due to its one-dimensional null space ($W\boldsymbol{\pi} = \mathbf{0}$ and $W\mathbf{e}^T = 0$), we should resort to the Drazin $W^{\mathcal{D}}$. Multiplying Eq. (27) by $W^{\mathcal{D}}$ on both sides, we obtain

$$\boldsymbol{\pi}' - \boldsymbol{\pi} = -W^{\mathcal{D}}(W' - W)\boldsymbol{\pi}', \quad (28)$$

where the property of Drazin pseudoinverse, $W^{\mathcal{D}}W = WW^{\mathcal{D}} = \mathbb{I} - \boldsymbol{\pi} \mathbf{e}$ has been used. We also use $\mathbf{e}(\boldsymbol{\pi}' - \boldsymbol{\pi}) = 0$ from normalization. Consider a minimal case when a single transition rate W_{ij} is perturbed to be W'_{ij} . In this case, the matrix $W' - W$ only has two non-zero entries $(W' - W)_{ij} = \Delta W_{ij}$ and $(W' - W)_{jj} = -\Delta W_{ij}$, which are both in the j -th column. Then, the k -th row of the matrix $-W^{\mathcal{D}}(W' - W)$ would be

$$[-W^{\mathcal{D}}(W' - W)]_k = (0 \cdots (W_{kj}^{\mathcal{D}} - W_{ki}^{\mathcal{D}}) \overset{j\text{-th element}}{\Delta W_{ij}} \cdots 0), \quad (29)$$

which has a single non-zero element, the j -th one. Consequently, the k -th element of the column vector $\boldsymbol{\pi}' - \boldsymbol{\pi}$ is

$$\begin{aligned} \pi'_k - \pi_k &= (W_{kj}^{\mathcal{D}} - W_{ki}^{\mathcal{D}}) \Delta W_{ij} \pi'_j \\ &= (\langle t_{kj} \rangle - \langle t_{ki} \rangle) \Delta W_{ij} \pi'_j \pi_k, \end{aligned} \quad (30)$$

where Eq. (25) has been used. For general cases, $[-W^{\mathcal{D}}(W' - W)]_k$ becomes

$$\left(\sum_{i=1}^N (W_{k1}^{\mathcal{D}} - W_{ki}^{\mathcal{D}}) \Delta W_{i1} \cdots \sum_{i=1}^N (W_{kj}^{\mathcal{D}} - W_{ki}^{\mathcal{D}}) \Delta W_{ij} \cdots \right). \quad (31)$$

That is, adding contributions from single transition rate perturbations up gives rise to Eq. (16). The duality equation Eq. (17) is obtained with the same procedure: we have

$$W'(\boldsymbol{\pi}' - \boldsymbol{\pi}) = -(W' - W)\boldsymbol{\pi}, \quad (32)$$

so that

$$\boldsymbol{\pi}' - \boldsymbol{\pi} = -W'^{\mathcal{D}}(W' - W)\boldsymbol{\pi}. \quad (33)$$

The derivation provided here is not limited to Markov jump processes. Generalization to the Fokker-Planck equation is possible, given that one can define a pseudoinverse of the Fokker-Planck operator, e.g., using the Green's function.

Appendix B: Multi-edge and global perturbation

For multi-edge perturbations, the upper bound for response precision can be obtained simply by adding the contributions from each single-edge together and using the triangle inequality, for instance,

$$\begin{aligned} \frac{|\sum_{e_{mn} \in S} \partial_{B_{mn}} \langle \mathcal{O} \rangle \pi|}{\sqrt{\text{Var}_{\boldsymbol{\pi}}(\mathcal{O})}} &\leq (1 - \frac{1}{N}) \sum_{e_{mn} \in S} \tanh(F_{\max}^{(m,n)}/4) \\ &\leq |S| (1 - \frac{1}{N}) \tanh(F_{\max}/4), \end{aligned} \quad (34)$$

where e_{mn} is the edge containing state m , n , and S is the set of edges being perturbed. Thus, the optimal response precision is at most of the order of the number $|S|$. One may also calculate the steady-state Fisher information matrix for multi-parameter $[I(\boldsymbol{\theta})]_{\mu\nu} = \sum_k \frac{\partial_{\theta_{\mu}} \pi_k \partial_{\theta_{\nu}} \pi_k}{\pi_k}$ and then use the multi-parameter Cramer-Rao inequality to obtain tighter bounds [15].

Additionally, on biological systems, sometimes global perturbations are more feasible to realize. A possible choice of global perturbation is $B_{ij}(b) \rightarrow B_{ij}(b+\epsilon)$, where b is a physical parameter associated with all edges and ϵ is a small perturbation on it. Then, the corresponding Fisher information is given by

$$I(b) = \sum_{e_{mn}} (\partial_b B_{mn})^2 I(B_{mn}) \leq b_{\max}^2 \sum_{e_{mn}} I(B_{mn}), \quad (35)$$

where e is the edge and $b_{max} := \max_e(\partial_b B_e)$. For such cases, the steady-state EPR can be bounded as

$$\dot{\sigma} \geq \frac{2(\min_{e_{mn}} A_{mn}) (\partial_b \langle \mathcal{O} \rangle_\pi)^2}{b_{max}^2 (1 - \frac{1}{N}) \text{Var}_\pi(\mathcal{O})}. \quad (36)$$

Other bounds in Eq. (10a)-(10c) and other types of global perturbation generalize similarly.

Appendix C: Response of normalized current observables

The normalized current observable $\langle \mathcal{J} \rangle^{nom} := \sum_{m < n} \mathcal{J}_{mn} (p_{mn} \pi_n - p_{nm} \pi_m)$ can be interpreted as the steady-state average of an observable \mathcal{J} over the joint probability distribution $p_{mn} \pi_n$: $\langle \mathcal{J} \rangle^{nom} = \sum_{m,n} \mathcal{J}_{mn} (p_{mn} \pi_n)$, with $\mathcal{J}_{mn} = -\mathcal{J}_{nm}$. Thus, to characterize the response behavior $\langle \mathcal{J} \rangle^{nom}$, we only need to analyze the response of $p_{mn} \pi_n$. For simplicity, we take the perturbation on B_{kl} as an illustrative example:

$$\frac{\partial(p_{mn} \pi_n)}{B_{kl}} = -(\langle t_{nl} \rangle - \langle t_{nk} \rangle) p_{mn} \pi_n j_{kl}, \quad (e_{mn} \neq e_{kl}) \quad (37)$$

$$\frac{\partial(p_{kl} \pi_l)}{B_{kl}} = p_{kl} \pi_l (-1 - p_{kl} + j_{kl} \langle t_{lk} \rangle). \quad (38)$$

Then, using Eq. (9a)-(9b), they can be upper bounded as

$$\left| \frac{\partial(p_{mn} \pi_n)}{B_{kl}} \right| \leq p_{mn} \pi_n \tanh(F_{max}^{(k,l)}/4) \leq p_{mn} \pi_n, \quad (39)$$

$$\left| \frac{\partial(p_{kl} \pi_l)}{B_{kl}} \right| \leq 2p_{kl} \pi_l. \quad (40)$$

Then, one can upper bound the Fisher information $I(B_{kl}) = \sum_{m,n} \left[\frac{\partial(p_{mn} \pi_n)}{B_{kl}} \right]^2 \frac{1}{p_{mn} \pi_n}$ associated with the probability distribution $p_{mn} \pi_n$ as

$$I(B_{kl}) \leq 1 + 3(p_{kl} \pi_l + p_{lk} \pi_k) \leq 4. \quad (41)$$

By the Cramer-Rao bound, the response precision is upper bounded as:

$$\frac{|\partial_{B_{mn}} \langle \mathcal{J} \rangle^{nom}|}{\sqrt{\text{Var}(\mathcal{J})}} \leq 2, \quad (42)$$

which is not related to activity. The steady-state variance is defined as $\text{Var}(\mathcal{J}) := \langle \mathcal{J}^2 \rangle^{nom} - (\langle \mathcal{J} \rangle^{nom})^2$, where the average is over $p_{mn} \pi_n$.

Appendix D: Additional response bound on finite perturbations

The Cramer-Rao inequality can be generalized to finite perturbation cases as [11]

$$\frac{|\langle \mathcal{O} \rangle_\pi^{\theta_1} - \langle \mathcal{O} \rangle_\pi^{\theta_0}|}{\sqrt{\text{Var}_\pi^{\theta_1}(\mathcal{O}) + \text{Var}_\pi^{\theta_0}(\mathcal{O})}} \leq \tanh\left(\frac{1}{2} \int_{\theta_0}^{\theta_1} \sqrt{I(\theta)} d\theta\right).$$

It leads to, for instance,

$$\frac{|\langle \mathcal{O} \rangle_\pi^{B'_e} - \langle \mathcal{O} \rangle_\pi^{B_e}|}{\sqrt{\text{Var}_\pi^{B'_e}(\mathcal{O}) + \text{Var}_\pi^{B_e}(\mathcal{O})}} \leq \tanh[(B'_e - B_e)(1 - \frac{1}{N})], \quad (43)$$

which demonstrates that activity does not contribute to the ultimate performance of response of state observables to strong perturbation.

-
- [1] R. Kubo, The fluctuation-dissipation theorem, Reports on Progress in Physics **29**, 255 (1966).
- [2] Y. Cao and S. Liang, Stochastic thermodynamics for biological functions, Quantitative Biology **13**, e75 (2025).
- [3] P. R. ten Wolde, N. B. Becker, T. E. Ouldridge, and A. Mugler, Fundamental Limits to Cellular Sensing, Journal of Statistical Physics **162**, 1395 (2016).
- [4] H. Qian, Phosphorylation Energy Hypothesis: Open Chemical Systems and Their Biological Functions, Annual Review of Physical Chemistry **58**, 113 (2007).
- [5] L. Peliti and S. Pigolotti, *Stochastic Thermodynamics: An Introduction* (Princeton University Press, 2021).
- [6] A. Dechant and S.-i. Sasa, Fluctuation-response inequality out of equilibrium, Proceedings of the National Academy of Sciences **117**, 6430 (2020).
- [7] J. A. Owen, T. R. Gingrich, and J. M. Horowitz, Universal Thermodynamic Bounds on Nonequilibrium Response with Biochemical Applications, Physical Review X **10**, 011066 (2020).
- [8] J. A. Owen, P. Talla, J. W. Biddle, and J. Gunawardena, Thermodynamic bounds on ultrasensitivity in covalent switching, Biophysical Journal **122**, 1833 (2023).
- [9] J. A. Owen and J. M. Horowitz, Size limits the sensitivity of kinetic schemes, Nature Communications **14**, 1280 (2023).
- [10] G. Fernandes Martins and J. M. Horowitz, Topologically constrained fluctuations and thermodynamics regulate nonequilibrium response, Physical Review E **108**, 044113 (2023).
- [11] Y. Hasegawa, Unifying speed limit, thermodynamic uncertainty relation and Heisenberg principle via bulk-boundary correspondence, Nature Communications **14**, 2828 (2023).
- [12] T. Aslyamov and M. Esposito, General Theory of Static Response for Markov Jump Processes, Physical Review Letters **133**, 107103 (2024).
- [13] T. Aslyamov and M. Esposito, Nonequilibrium Response for Markov Jump Processes: Exact Results and Tight Bounds, Physical Review Letters **132**, 037101 (2024).

- [14] K. Ptaszyński, T. Aslyamov, and M. Esposito, Dissipation Bounds Precision of Current Response to Kinetic Perturbations, *Physical Review Letters* **133**, 227101 (2024).
- [15] E. Kwon, H.-M. Chun, H. Park, and J. S. Lee, Fluctuation-response inequalities for kinetic and entropic perturbations (2024), arXiv:2411.18108 [cond-mat].
- [16] P. E. Harunari, S. Dal Cengio, V. Lecomte, and M. Poletini, Mutual Linearity of Nonequilibrium Network Currents, *Physical Review Letters* **133**, 047401 (2024).
- [17] Y. Hasegawa, Thermodynamic Correlation Inequality, *Physical Review Letters* **132**, 087102 (2024).
- [18] C. Maes, Response Theory: A Trajectory-Based Approach, *Frontiers in Physics* **8**, 229 (2020).
- [19] K. Liu and J. Gu, Dynamical activity universally bounds precision of response (2024), arXiv:2410.20800 [cond-mat].
- [20] J. Zheng and Z. Lu, Universal Non-equilibrium Response Theory Beyond Steady States (2024), arXiv:2403.10952 [cond-mat].
- [21] G. Lan, P. Sartori, S. Neumann, V. Sourjik, and Y. Tu, The energy–speed–accuracy trade-off in sensory adaptation, *Nature Physics* **8**, 422 (2012).
- [22] Y. Tu and W.-J. Rappel, Adaptation in living systems, *Annual review of condensed matter physics* **9**, 183 (2018).
- [23] U. Seifert, From Stochastic Thermodynamics to Thermodynamic Inference, *Annual Review of Condensed Matter Physics* **10**, 171 (2019).
- [24] P. E. Harunari, A. Dutta, M. Poletini, and E. Roldán, What to learn from a few visible transitions’ statistics?, *Phys. Rev. X* **12**, 041026 (2022).
- [25] J. van der Meer, B. Ertel, and U. Seifert, Thermodynamic inference in partially accessible markov networks: A unifying perspective from transition-based waiting time distributions, *Phys. Rev. X* **12**, 031025 (2022).
- [26] C. D. Meyer, Jr., The Condition of a Finite Markov Chain and Perturbation Bounds for the Limiting Probabilities, *SIAM Journal on Algebraic Discrete Methods* **1**, 273 (1980).
- [27] G. E. Cho and C. D. Meyer, Markov chain sensitivity measured by mean first passage times, *Linear Algebra and its Applications* **316**, 21 (2000).
- [28] S. E. Harvey, S. Lahiri, and S. Ganguli, Universal energy-accuracy tradeoffs in nonequilibrium cellular sensing, *Physical Review E* **108**, 014403 (2023).
- [29] A. C. Barato and U. Seifert, Thermodynamic Uncertainty Relation for Biomolecular Processes, *Physical Review Letters* **114**, 158101 (2015).
- [30] T. R. Gingrich, J. M. Horowitz, N. Perunov, and J. L. England, Dissipation bounds all steady-state current fluctuations, *Phys. Rev. Lett.* **116**, 120601 (2016).
- [31] J. M. Horowitz and T. R. Gingrich, Proof of the finite-time thermodynamic uncertainty relation for steady-state currents, *Phys. Rev. E* **96**, 020103 (2017).
- [32] P. Pietzonka, F. Ritort, and U. Seifert, Finite-time generalization of the thermodynamic uncertainty relation, *Phys. Rev. E* **96**, 012101 (2017).
- [33] A. Dechant, Multidimensional thermodynamic uncertainty relations, *Journal of Physics A: Mathematical and Theoretical* **52**, 035001 (2018).
- [34] Y. Hasegawa and T. Van Vu, Uncertainty relations in stochastic processes: An information inequality approach, *Phys. Rev. E* **99**, 062126 (2019).
- [35] K. Liu, Z. Gong, and M. Ueda, Thermodynamic uncertainty relation for arbitrary initial states, *Phys. Rev. Lett.* **125**, 140602 (2020).
- [36] C. Dieball and A. c. v. Godec, Direct route to thermodynamic uncertainty relations and their saturation, *Phys. Rev. Lett.* **130**, 087101 (2023).
- [37] F. Khodabandehlou, C. Maes, and K. Netočný, Affine relationships between steady currents (2024), arXiv:2412.05019 [cond-mat].
- [38] K. Ptaszynski, T. Aslyamov, and M. Esposito, Nonequilibrium Fluctuation-Response Relations for State Observables (2024), arXiv:2412.10233 [cond-mat].
- [39] C. C. Govern and P. R. Ten Wolde, Energy Dissipation and Noise Correlations in Biochemical Sensing, *Physical Review Letters* **113**, 258102 (2014).
- [40] G. Nicoletti and D. M. Busiello, Information propagation in multilayer systems with higher-order interactions across timescales, *Phys. Rev. X* **14**, 021007 (2024).
- [41] G. Nicoletti, M. Bruzzone, S. Suweis, M. Dal Maschio, and D. M. Busiello, Information gain at the onset of habituation to repeated stimuli, *eLife* **13**, 10.7554/eLife.99767.1 (2024).
- [42] D. D. Yao, First-passage-time moments of Markov processes, *Journal of Applied Probability* **22**, 939 (1985).
- [43] S. L. Campbell and C. D. Meyer, *Generalized Inverses of Linear Transformations* (SIAM, 2009).
- [44] K. Ptaszynski and M. Esposito, Critical heat current fluctuations in Curie-Weiss model in and out of equilibrium (2024), arXiv:2411.19643 [cond-mat].